Quantitative assessment of corpus callosum morphology in periventricular nodular heterotopia

Heath R. Pardoe[1], **Simone A. Mandelstam**[2], **Rebecca Kucharsky Hiess**[1], **Ruben I. Kuzniecky**[1], **Graeme D. Jackson**[2], **Alzheimer's Disease Neuroimaging Initiative**[*], and **Epilepsy Phenome/Genome Project Investigators**[**]

[1]Comprehensive Epilepsy Center, Department of Neurology, New York University School of Medicine, New York, NY

[2]Florey Institute of Neuroscience and Mental Health, Melbourne, Australia

Abstract

We investigated systematic differences in corpus callosum morphology in periventricular nodular heterotopia (PVNH). Differences in corpus callosum mid-sagittal area and subregional area changes were measured using an automated software-based method. Heterotopic gray matter deposits were automatically labeled and compared with corpus callosum changes. The spatial pattern of corpus callosum changes were interpreted in the context of the characteristic anterior-posterior development of the corpus callosum in healthy individuals.

Individuals with periventricular nodular heterotopia were imaged at the Melbourne Brain Center or as part of the multi-site Epilepsy Phenome Genome project. Whole brain T1 weighted MRI was acquired in cases (n = 48) and controls (n = 663). The corpus callosum was segmented on the mid-sagittal plane using the software "yuki". Heterotopic gray matter and intracranial brain volume was measured using Freesurfer. Differences in corpus callosum area and subregional areas were assessed, as well as the relationship between corpus callosum area and heterotopic GM volume. The anterior-posterior distribution of corpus callosum changes and heterotopic GM nodules were quantified using a novel metric and compared with each other.

Corpus callosum area was reduced by 14% in PVNH (p = 1.59×10^{-9}). The magnitude of the effect was least in the genu (7% reduction) and greatest in the isthmus and splenium (26% reduction). Individuals with higher heterotopic GM volume had a smaller corpus callosum. Heterotopic GM volume was highest in posterior brain regions, however there was no linear relationship between the anterior-posterior position of corpus callosum changes and PVNH nodules.

Reduced corpus callosum area is strongly associated with PVNH, and is probably associated with abnormal brain development in this neurological disorder. The primarily posterior corpus callosum changes may inform our understanding of the etiology of PVNH. Our results suggest that interhemispheric pathways are affected in PVNH.

Keywords

Epilepsy; Neuroimaging; Brain Development; MRI

1. Introduction

Abnormalities of the corpus callosum, including hypoplasia, dysgenesis or agenesis, have been reported in individuals with periventricular nodular heterotopia (Parrish, Roessmann et al. 1979, Barkovich and Norman 1988, Pisano, Barkovich et al. 2012, Mandelstam, Leventer et al. 2013). We applied a recently developed method for segmenting the corpus callosum using a T1-weighted MRI scan to individuals with periventricular nodular heterotopia, in order to quantitatively assess if corpus callosum morphology is affected in individuals without agenesis or obvious dysgenesis. An automated labeling method was used to label heterotopic GM deposits and the relationship between heterotopic GM volume and corpus callosum morphology was investigated. Comparison of corpus callosum area and the volume of heterotopic GM will allow us to determine if the abnormal developmental processes giving rise to heterotopic GM nodules may also interfere with the formation of interhemispheric connections.

We also present novel methods for quantifying the anterior-posterior distribution of corpus callosum changes and heterotopic gray matter nodules. These methods were used to compare the anterior-posterior distribution of corpus callosum changes with the anterior-posterior location of heterotopic gray matter nodules. The position of corpus callosum changes may be relevant for investigating the etiology of periventricular nodular heterotopia, since the corpus callosum develops in a generally anterior-posterior direction, with the genu forming earliest and the splenium developing later (Rakic and Yakovlev 1968). The exception to this pattern of development is the formation of the rostrum of the corpus callosum, which is last. If there is a spatial pattern of corpus callosum changes in individuals with periventricular nodular heterotopia, we may be able to infer when normal development was disrupted and formation of heterotopic gray matter nodules occurred.

Specific hypotheses tested in this study were:

1. Corpus callosum area will be different in individuals with periventricular nodular heterotopia relative to healthy controls.

2. The volume of tissue labeled using an automated software-based method will be increased in individuals with PVNH & qualitatively correspond to heterotopic GM nodules.

3. There will be a relationship between corpus callosum area and the volume of heterotopic GM in individuals with PVNH.

4. The anterior-posterior distribution of corpus callosum changes will be related to the anterior-posterior distribution of heterotopic GM.

2. Methods

2.1 Participant recruitment and imaging

Two groups of individuals with periventricular nodular heterotopia (PNH) were included in this study. The first group were individuals imaged at the Melbourne Brain Center, Austin Hospital, Melbourne consecutively between 2009–2013. The second group of individuals with PNH were recruited as part of the Epilepsy Phenome/Genome Project (EPGP) cohort, a multicentre collaborative epilepsy study (Abou-Khalil, Alldredge et al. 2013). PNH subjects were included if they (i) had heterotopic GM nodules observed on their MRI scan and (ii) the MRI scan was of sufficient quality for processing using the corpus callosum segmentation software. Melbourne MRI acquisition parameters: T1-weighted whole-brain MRI was acquired on a 3 T Siemens TIM Trio MRI scanner with the following acquisition parameters: TR = 1900 ms, TI = 900 ms, TE = 2.6 ms, flip angle = 9°, voxel resolution = 0.9 mm isotropic. EPGP MRI acquisition parameters were variable depending on each sites epilepsy imaging or clinical imaging protocol. Each EPGP participant included in our analysis had a whole brain T1-weighted MRI scan acquired at 1.5T (n = 19) or 3T (n = 22), with in-plane voxel size ranging from 0.42–1 mm and slice thickness range 1–2 mm, with an average voxel volume of 0.91 mm^3. Because the EPGP dataset consisted of a combination of 3T and 1.5T imaging data, a supplementary analysis was carried out using a ADNI control data in which ADNI controls scanned at 1.5T were compared with ADNI controls scanned at 3T. The purpose of this analysis was to determine if there are systematic differences between corpus callosum mid-sagittal area measured at 1.5T compared with 3T. Data used in this supplementary analysis were obtained from the Alzheimer's Disease Neuroimaging Initiative (ADNI) database (adni.loni.usc.edu).

A large multi-site group of control MRI scans were used to provide normative corpus callosum morphology data, to account for the multiple scanners used in the EPGP study. The primary control group consisted of co-workers and colleagues from the Melbourne Brain Center, Austin Hospital, Melbourne. A second multi-site control group was obtained by selecting control MRI scans from the ABIDE study MRI dataset (Di Martino, Yan et al 2014, http://fcon_1000.projects.nitrc.org/indi/abide/). Acquisition details for each site in the ABIDE study are provided as supplementary material. Control subjects were neurologically healthy with no known neurological disorders. All participants provided informed consent to participate in the study.

2.2 Image processing

The corpus callosum was segmented using the software package "yuki" (version 2.1, Ardekani 2013, Figure 1). Corpus callosum segmentations occasionally required manual input to improve segmentation accuracy. Manual edits were carried out blind to subject classification. Total corpus callosum mid-sagittal area and regional areas were derived using the Witelson subdivision scheme, which parcellates the corpus callosum into 7 regions along the anterior-posterior axis (Witelson 1989, Figure 1). As described in Witelson, the rostrum of the corpus callosum corresponds to region W1, the genu is region W2, rostral body is region W3, anterior and posterior midbody regions are W4 and W5 respectively, W6 is the isthmus and W7 corresponds to the splenium.

Structural MRI scans were processed using the subcortical processing stream carried out as part of default brain processing stream using Freesurfer version 5.3 (Fischl, Salat et al. 2002). The label "white matter hypointensity" was investigated with respect to labelling heterotopic GM nodules. In addition to the white matter hypointensity label, total white matter volume and total intracranial volume were derived from the Freesurfer image processing pipeline.

Differences in corpus callosum mid-sagittal area between cases and controls were assessed using a general linear model, with age, gender and brain volume included as covariates. Analyses were conducted with (i) Melbourne PVNH and control data alone, and (ii) Melbourne and EPGP PVNH data compared with Melbourne and ABIDE control data (i.e. all data pooled). The purpose of these separate analyses was to determine the validity of including the EPGP PNH group in the absence of site-matched controls for these participants. The ABIDE control data was only used for this statistical analysis and was not used in any further analyses described in this study. Cohen's d was calculated to provide a measure of the strength of any detected difference. A post-hoc comparison of corpus callosum area was carried out with white matter volume instead of brain volume to determine if overall white matter volume differences were responsible for detected differences in corpus callosum area in PVNH.

ADNI control MRI data obtained at 1.5T and 3T was compared using a general linear model with age, gender and brain volume included as additional covariates. The ADNI analysis was included to determine if field strength differences could potentially introduce systematic differences in the EPGP patient cohort. Given the older age of ADNI participants, this control data was only used to address the field strength question and was not used in any comparisons with epilepsy participants.

In order to determine if the white matter hypointensity label measures heterotopic GM, differences in this label between PVNH participants and healthy controls were investigated using a general linear model. Age, gender and brain volume were included as covariates. Images were visually inspected to assess the accuracy of heterotopic GM labelling. The relationship between corpus callosum area and volume of heterotopic GM was investigated using a general linear model with corpus callosum area as the dependent variable and white matter hypointensity volume (as an index of the volume of heterotopic GM), age, gender and brain volume as independent variables.

2.3 Quantification of anterior-posterior distribution of PVNH & corpus callosum changes

The white matter hypointensity label derived from Freesurfer was coregistered to MNI space by (i) deriving a rigid body transformation mapping the structural MRI to an MNI-152 1mm template brain provided with the FSL software package (Jenkinson and Smith 2001), and (ii) applying the transform to the white matter hypointensity label. The area of the WM hypointensity label in each slice along the anterior-posterior axis was measured (Figure 2). This process was applied to all subjects in the study (patients + controls). A metric summarizing the mean anterior-posterior position of the heterotopic GM deposits was derived by: i) measuring the 95th percentile of the WM hypointensity label in each slice in healthy controls and ii) subtracting this value from the measured area of WM hypointensity for each patient. In this way we identified slices with excess heterotopic GM in each individual with PVNH relative to the majority of controls. The mean position of the heterotopic GM was then assessed by measuring the mean y-value weighted by the area of heterotopic GM in each slice. We refer to this metric as $PVNH_{ant-pos}$. $PVNH_{ant-pos}$ was compared with qualitative estimates of heterotopic GM distribution by visually classifying EPGP PVNH MRI scans as "anterior" for individuals with predominantly anterior nodules, "trigonal" with predominantly trigonal nodules or "distributed" when heterotopic GM was distributed along the length of the ventricles. The comparison of the quantitative metric and visual inspection was carried out using the general linear model. We expected scans labelled as "anterior" to have higher values of $PVNH_{ant-pos}$, cases labelled as "distributed" to have intermediate values and trigonal cases to have lower values of $PVNH_{ant-pos}$.

A similar process was used to derive a single value that summarized the position of corpus callosum changes. Regional corpus callosum areas were corrected for brain volume and age, and z-scores measured for each individual with PVNH in each Witelson subregion. The mean position of corpus callosum changes was measured by weighting the mean position (i.e. 1–7) by the z-score in each region. We refer to this metric as $CC_{ant-pos}$. Witelson region 4 corresponds to the mid-body of the corpus callosum; therefore if $CC_{ant-pos}$ is less than 4 corresponds reduced area predominantly located in anterior corpus callosum regions, and a value greater than 4 corresponds to reduced area in posterior corpus callosum regions. $CC_{ant-pos}$ and $PVNH_{ant-pos}$ were compared using linear regression to determine if the anterior-posterior location of heterotopic GM is related to the position of corpus callosum changes along the length of the structure.

3. Results

48 individuals with PNH were included in the study (32 female, mean age 27.8 ± 13.6 years). 14 subjects were included from the Austin Hospital, Melbourne. Eleven individuals in this group had epilepsy, two subjects were asymptomatic relatives of a proband with FLNA mutation, and one individual was a healthy volunteer with an incidental finding of nodules. 34 subjects with epilepsy were included from the EPGP study. Four EPGP participants had learning difficulties. No individuals in this study had corpus callosum agenesis. One EPGP participant had an absent splenium, based on visual inspection of MRI. The Melbourne control group was comprised of 98 healthy controls (52 female, mean age

29.5 ± 9.8 years). The ABIDE study control group consisted of 565 healthy controls (97 female, mean age 17.08 ± 7.7 years).

The ADNI control MRI group consisted of 80 1.5T MRI scans (45 female, mean age 78.3 ± 5.1 years) and 46 3T MRI scans (30 female, 77.9 ± 5.1 years). Comparison of corpus callosum area estimates provided no evidence for systematic differences due to MRI field strength (0.46% difference between groups, p = 0.82).

Mean corpus callosum mid-sagittal area was 14.3% smaller in PNH compared to healthy controls (Figure 3, p = 1.59×10^{-9} after controlling for brain volume, age and gender). Cohen's d was 0.8, which is traditionally accepted as a large effect. Separating the PNH data into Melbourne and EPGP groups and (i) comparing Melbourne PVNH with Melbourne controls and (ii) comparing multi-site EPGP PVNH with multi-site control MRI indicated a similar pattern of reduced corpus callosum area with variable magnitude of the effect (Melbourne, 23% decrease, p = 1.25×10^{-8}; EPGP, 10.2% decrease, p = 1.7×10^{-4}). The high value of Cohen's d indicates that the strength of the detected effect overcomes any increased variance or systematic differences introduced by the use of multiple scanners for imaging the EPGP participants; this variance may explain the site-related difference in magnitude of the area decrease.

Corpus callosum changes in PVNH were investigated in each of the Witelson subregions by conducting separate analyses of the area of each Witelson subdivision W1–W7 as dependent variables, and diagnosis, brain volume, age and gender as independent variables. Corpus callosum area was reduced along the length of the corpus callosum, with progressively increasing magnitude of reduced area in an anterior to posterior direction, with the greatest reduction in the splenium (Figure 3, p values for W1–W7 in order: 0.04, 0.05, 0.003, 3.79×10^{-5}, 8.61×10^{-7}, 3.18×10^{-8}, 3.03×10^{-14}).

A post-hoc analysis of overall corpus callosum area changes in PVNH was conducted with white matter volume included as an independent variable instead of total brain volume; the difference in corpus callosum area remained highly significant (p = 4.46×10^{-9}). This indicates that the corpus callosum changes we identified are specific to the corpus callosum and not driven by an overall change in white matter volume, which has been reported in previous studies (Walker, Katzir et al. 2009, Gonzalez, Vedolin et al. 2013).

Comparison of the white matter hypointensity label indicated significantly increased volume in PVNH participants relative to controls (p = 7.61×10^{-16}). White matter hypointensity volume was 5304 ± 4248 mm^3 in PVNH participants, and 1231 ± 565 mm^3 in healthy controls. Visual inspection confirmed that heterotopic GM nodules were labelled as "white matter hypointensity" by Freesurfer, although coverage was occasionally incomplete, particularly in individuals with large heterotopic GM deposits (see anterior heterotopic nodules in Figure 2). Because the label was not zero in controls, and incomplete in some cases, the label is not 100% sensitive or specific to PVNH. Nevertheless the very high significance of the quantitative analysis and visual inspection suggested that the white matter hypointensity label was a good index of heterotopic GM volume in PVNH.

Heterotopic GM volume (as indexed using the white matter hypointensity label) was a significant predictor of corpus callosum area (-1.55×10^{-2} mm^2 cc per mm^3 PVNH volume, p = 3.18×10^{-8}), which indicates that individuals with more heterotopic GM have a smaller corpus callosum (Figure 4).

Comparison of our novel quantitative metric "PVNH$_{ant-pos}$" with visual assessment indicated that the quantitative values agreed with visual assessment of the distribution of heterotopic GM nodules. Individuals with MRI scans assessed as having anterior PVNH had a mean PVNH$_{ant-pos}$ = 0 (corresponding to the coronal plane containing the anterior commissure on the MNI template brain); individuals assessed as having distributed PVNH nodules had a mean PVNH$_{ant-pos}$ = −28 (significantly less than anterior PVNH cases, p = 0.011) and individuals with trigonal PVNH nodules had mean PVNH$_{ant-pos}$ = −45, p = 1.38×10^{-4}.

The highest volume of heterotopic GM was located in a posterior region around MNI coordinate y = −50, and an additional anterior volume peak was located at approximately y = +25 (Figure 5). Although individuals with higher volumes of heterotopic GM have smaller corpus callosum area, and both corpus callosum area and heterotopic GM changes are primarily located posteriorly, no linear relationship between the location of corpus callosum atrophy and heterotopic GM location along the posterior axis was identified (Figure 6, p = 0.92). As indicated in Figure 6, an individual may have heterotopic GM deposits along the length of the anterior-posterior axis but will typically have posterior corpus callosum atrophy.

Quantitative data and instructions for recreating statistical analyses and plots are provided at the following web site: https://sites.google.com/site/hpardoe/periventricular.

4. Discussion

We have used quantitative methods to demonstrate that there are systematic reductions in corpus callosum mid-sagittal area associated with periventricular nodular heterotopia. Differences exist along the length of the corpus callosum, but the magnitude of the effect appears to follow an anterior-posterior direction, with the greatest area reduction in the isthmus and splenium of the corpus callosum. The magnitude of the corpus callosum area reduction is related to the volume of heterotopic grey matter in each individual; people with higher volume of heterotopic grey matter have a smaller corpus callosum. This observation suggests that interhemispheric white matter pathway development is disrupted in individuals with PVNH.

We have found that both corpus callosum changes and heterotopic GM deposition are primarily posterior, as has been previously reported (Mandelstam et al 2013). Our analyses suggest that the anterior-posterior location of heterotopic grey matter does not directly translate to the location of corpus callosum atrophy. More sophisticated methods for mapping white matter using diffusion imaging may assist in characterizing the spatial relationship between the pattern of heterotopic GM deposition and white matter changes.

As noted in a previous study by Barkovich et al (Barkovich and Norman 1988), corpus callosum morphometric properties may provide information for determining if neurological insults occurred during in utero or perinatal periods of development. Given that the period for maximum growth of the splenium occurs after more anterior parts of the corpus callosum (Rakic and Yakovlev 1968), a potential interpretation of our findings is that individuals with more posterior corpus callosum changes had abnormal developmental changes (i.e. development of heterotopic GM) later than individuals with more anterior corpus callosum changes. This hypothesis is supported by previously published findings in temporal lobe epilepsy that found that patients with earlier epilepsy onset had more anterior corpus callosum changes (Weber, Luders et al. 2007). It is interesting that a similar pattern of corpus callosum changes was reported in this study, with predominantly posterior changes in the temporal lobe epilepsy group.

The question remains whether the observed corpus callosum changes are developmental in origin or are the result of ongoing seizures. Because we did not investigate seizure frequency or age of seizure onset in relation to corpus callosum morphology, our study does not answer this question. Previous studies that investigate this issue tend to suggest a neurodevelopmental origin. Hermann et al identified a similar pattern of corpus callosum changes in individuals with early onset temporal lobe epilepsy, with more severe posterior changes than anterior changes compared with both healthy controls and late onset cases (Hermann, Hansen et al. 2003). A recently published diffusion imaging study that investigated corpus callosum changes in individuals with malformations of cortical development did not identify a relationship between corpus callosum diffusion changes and age of epilepsy onset or epilepsy duration, which they interpreted as suggesting a developmental origin for corpus callosum changes (Andrade, Leite et al. 2014).

The method we used for quantification of heterotopic grey matter nodules is freely available, and provides an alternative approach to a recently published technique (Pascher, Kroll et al. 2013). As noted in the results section, labelling was occasionally incomplete in severe cases. It is unclear which method is best for labelling nodules, however the novel method we presented for quantifying the anterior-posterior distribution of heterotopic grey matter could be easily applied to any method for labelling heterotopic GM.

In summary, we have used quantitative analysis to demonstrate that periventricular nodular heterotopia is associated with reduced corpus callosum area. The large effect size reported in this study supports the hypothesis that abnormal corpus callosum morphology is a common feature of periventricular nodular heterotopia, in addition to previously reported changes in temporal lobe epilepsy and malformations of cortical development. The novel methods we have presented for mapping the spatial distribution of structural changes may provide additional information that could be useful for characterizing heterotopia subtypes, and may also be useful for quantitative assessment of corpus callosum morphology in other epilepsy syndromes and neurological disorders.

Acknowledgments

References

Abou-Khalil B, Alldredge B, Bautista J, Berkovic S, Bluvstein J, Boro A, Cascino G, Consalvo D, Cristofaro S, Crumrine P, Devinsky O, Dlugos D, Epstein M, Fahlstrom R, Fiol M, Fountain N, Fox K, French J, Freyer Karn C, Friedman D, Geller E, Glauser T, Glynn S, Haut S, Hayward J, Helmers S, Joshi S, Kanner A, Kirsch H, Knowlton R, Kossoff E, Kuperman R, Kuzniecky R, Lowenstein D, McGuire S, Motika P, Nesbitt G, Novotny E, Paolicchi J, Parent J, Park K, Poduri A, Risch N, Sadleir L, Scheffer I, Shellhaas R, Sherr E, Shih JJ, Shinnar S, Singh R, Sirven J, Smith M, Sullivan J, Thio LL, Venkat A, Vining E, von Allmen G, Weisenberg J, Widdess-Walsh P, Winawer M. The epilepsy phenome/genome project. Clin Trials. 2013; 10(4):568–586. [PubMed: 23818435]

Andrade CS, Leite CC, Otaduy MC, Lyra KP, Valente KD, Yasuda CL, Beltramini GC, Beaulieu C, Gross DW. Diffusion abnormalities of the corpus callosum in patients with malformations of cortical development and epilepsy. Epilepsy Res. 2014

Ardekani BA. yuki module of the Automatic Registration Toolbox (ART) for corpus callosum segmentation. 2013

Barkovich AJ, Norman D. Anomalies of the corpus callosum: correlation with further anomalies of the brain. AJR Am J Roentgenol. 1988; 151(1):171–179. [PubMed: 3259802]

Di Martino A, Yan CG, Li Q, Denio E, Castellanos FX, Alaerts K, Anderson JS, Assaf M, Bookheimer SY, Dapretto M, Deen B, Delmonte S, Dinstein I, Ertl-Wagner B, Fair DA, Gallagher L, Kennedy DP, Keown CL, Keysers C, Lainhart JE, Lord C, Luna B, Menon V, Minshew NJ, Monk CS, Mueller S, Muller RA, Nebel MB, Nigg JT, O'Hearn K, Pelphrey KA, Peltier SJ, Rudie JD, Sunaert S, Thioux M, Tyszka JM, Uddin LQ, Verhoeven JS, Wenderoth N, Wiggins JL, Mostofsky SH, Milham MP. The autism brain imaging data exchange: towards a large-scale evaluation of the intrinsic brain architecture in autism. Mol Psychiatry. 2014; 19(6):659–667. [PubMed: 23774715]

Fischl B, Salat DH, Busa E, Albert M, Dieterich M, Haselgrove C, van der Kouwe A, Killiany R, Kennedy D, Klaveness S, Montillo A, Makris N, Rosen B, Dale AM. Whole brain segmentation: automated labeling of neuroanatomical structures in the human brain. Neuron. 2002; 33(3):341–355. [PubMed: 11832223]

Gonzalez G, Vedolin L, Barry B, Poduri A, Walsh C, Barkovich AJ. Location of periventricular nodular heterotopia is related to the malformation phenotype on MRI. AJNR Am J Neuroradiol. 2013; 34(4):877–883. [PubMed: 23064591]

Hermann B, Hansen R, Seidenberg M, Magnotta V, O'Leary D. Neurodevelopmental vulnerability of the corpus callosum to childhood onset localization-related epilepsy. Neuroimage. 2003; 18(2):284–292. [PubMed: 12595183]

Jenkinson M, Smith S. A global optimisation method for robust affine registration of brain images. Med Image Anal. 2001; 5(2):143–156. [PubMed: 11516708]

Mandelstam SA, Leventer RJ, Sandow A, McGillivray G, van Kogelenberg M, Guerrini R, Robertson S, Berkovic SF, Jackson GD, Scheffer IE. Bilateral posterior periventricular nodular heterotopia: a recognizable cortical malformation with a spectrum of associated brain abnormalities. AJNR Am J Neuroradiol. 2013; 34(2):432–438. [PubMed: 23348762]

Parrish ML, Roessmann U, Levinsohn MW. Agenesis of the corpus callosum: a study of the frequency of associated malformations. Ann Neurol. 1979; 6(4):349–354. [PubMed: 554524]

Pascher B, Kroll J, Mothersill I, Kramer G, Huppertz HJ. Automated morphometric magnetic resonance imaging analysis for the detection of periventricular nodular heterotopia. Epilepsia. 2013; 54(2):305–313. [PubMed: 23330738]

Pisano T, Barkovich AJ, Leventer RJ, Squier W, Scheffer IE, Parrini E, Blaser S, Marini C, Robertson S, Tortorella G, Rosenow F, Thomas P, McGillivray G, Andermann E, Andermann F, Berkovic SF, Dobyns WB, Guerrini R. Peritrigonal and temporo-occipital heterotopia with corpus callosum and cerebellar dysgenesis. Neurology. 2012; 79(12):1244–1251. [PubMed: 22914838]

Rakic P, Yakovlev PI. Development of the corpus callosum and cavum septi in man. J Comp Neurol. 1968; 132(1):45–72. [PubMed: 5293999]

Walker LM, Katzir T, Liu T, Ly J, Corriveau K, Barzillai M, Chu F, O'Connor MG, Hackney DB, Chang BS. Gray matter volumes and cognitive ability in the epileptogenic brain malformation of periventricular nodular heterotopia. Epilepsy Behav. 2009; 15(4):456–460. [PubMed: 19541546]

Weber B, Luders E, Faber J, Richter S, Quesada CM, Urbach H, Thompson PM, Toga AW, Elger CE, Helmstaedter C. Distinct regional atrophy in the corpus callosum of patients with temporal lobe epilepsy. Brain. 2007; 130(Pt 12):3149–3154. [PubMed: 17728360]

Witelson SF. Hand and sex differences in the isthmus and genu of the human corpus callosum. A postmortem morphological study. Brain. 1989; 112(Pt 3):799–835. [PubMed: 2731030]

Highlights (for review)

- Corpus callosum area reduced by 14% in periventricular nodular heterotopia

- Area reduction varies from 7% in genu to 25% in isthmus and splenium

- Most heterotopic GM in posterior brain regions

- No linear relationship between position of corpus callosum atrophy & heterotopic GM
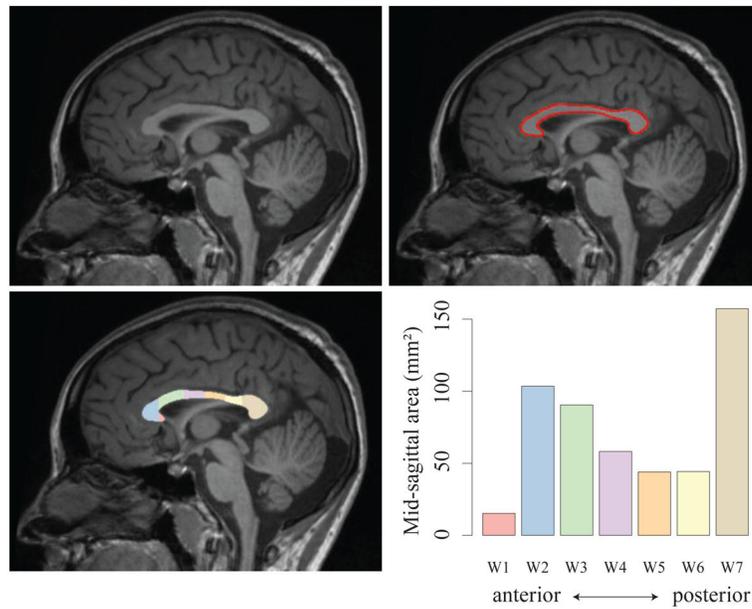
Figure 1.
Corpus callosum segmentation using T1-weighted MRI. The mid-sagittal plane is identified (A), corpus callosum is segmented (B) and subdivided according to the Witelson scheme (C). The cross-sectional area of each Witelson subregion is shown in D. Total cross-sectional area for this individual is 513 mm2.
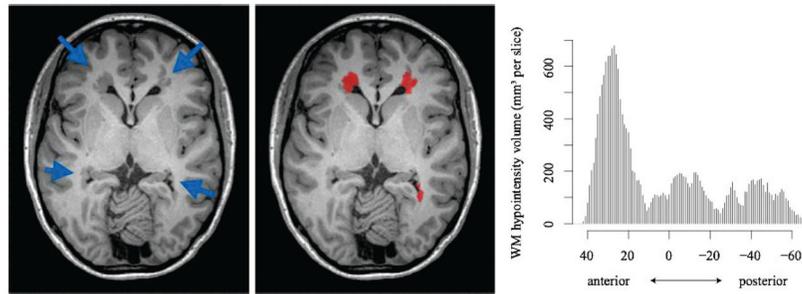
Figure 2.
Heterotopic GM labelling. A. Axial slice showing heterotopic GM nodules primarily located in anterior regions (blue arrows). B. Freesurfer-based labelling of PVNH nodules C. Anterior-posterior distribution of heterotopic GM indicates primarily anterior heterotopic GM in this individual. The x-axis on the bar chart indicates y-coordinates in MNI space.
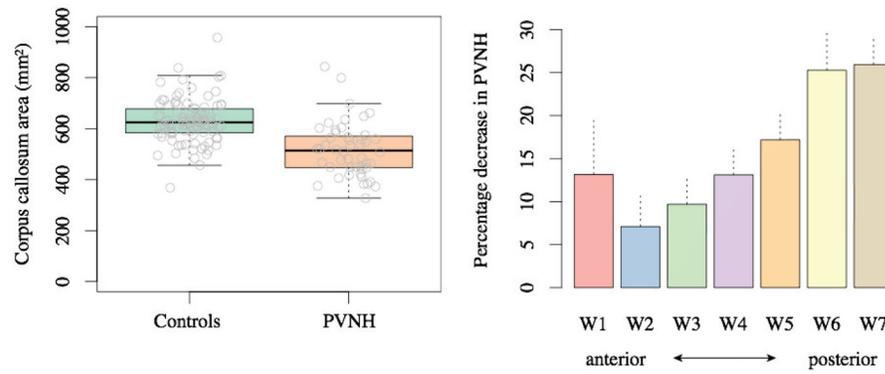
Figure 3.
Corpus callosum area is reduced in individuals with PVNH (p = 1.59 × 10^{-9}). Individual values are plotted as grey circles (A). Corpus callosum area values have been corrected for brain volume & additional covariates. Differences between PVNH participants and controls in Witelson subregions indicate that the effect is strongest in posterior corpus callosum (B). Note that region W2 (genu) is formed earliest in healthy individuals, with regions W3–W7 formed sequentially and region W1 (rostrum) formed last. Dashed lines indicate standard errors of the mean.
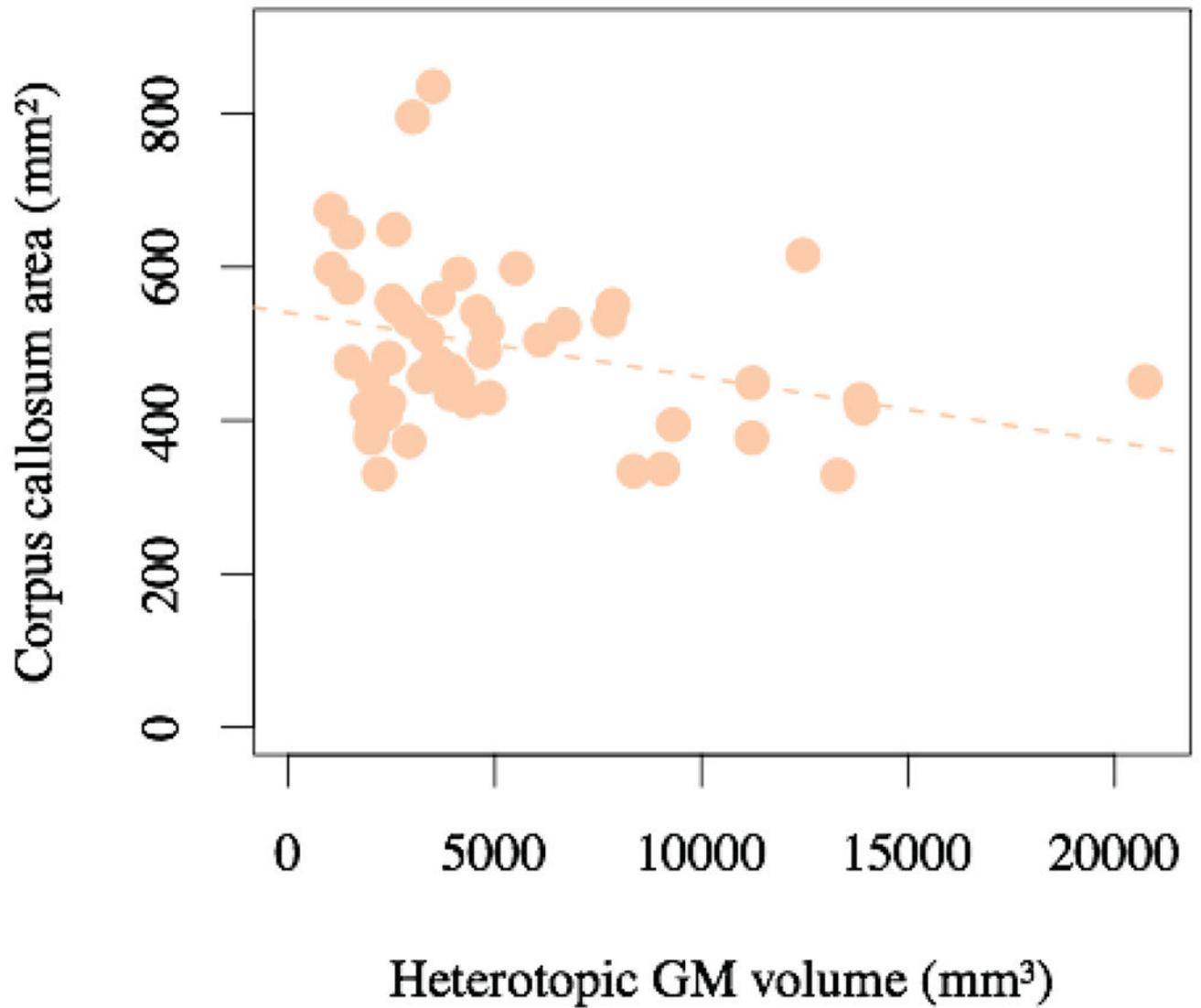
Figure 4.
Individuals with higher heterotopia volume have a smaller corpus callosum ($p = 3.2 \times 10^{-8}$ after controlling for covariates, R2 = 0.33, orange dashed line).
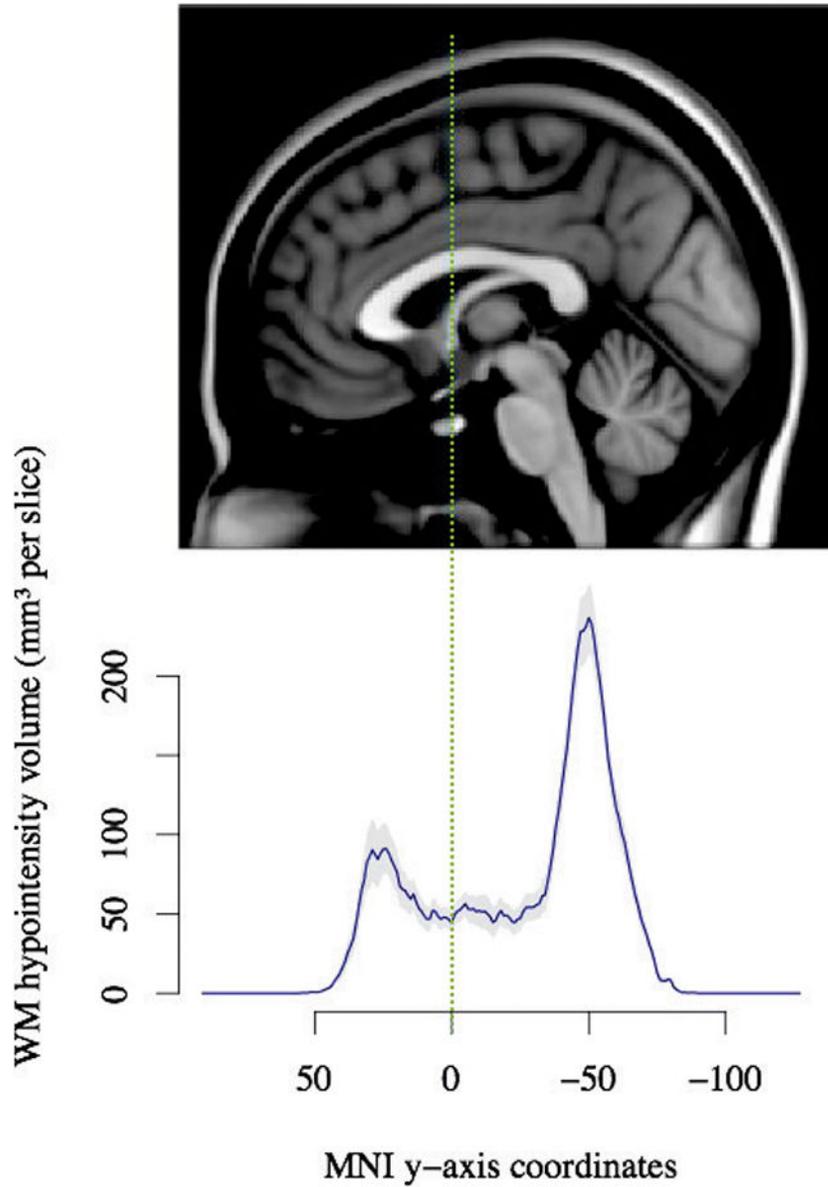
Figure 5.
Anterior-posterior distribution of heterotopic grey matter. The plot indicates that heterotopic GM is particularly high in posterior regions. The MRI slice is the midsagittal slice of the MNI-152 brain template. The solid line indicates the average difference in white matter hypointensity labels between PVNH participants and controls after controlling for covariates and dashed lines indicate standard error of the mean.
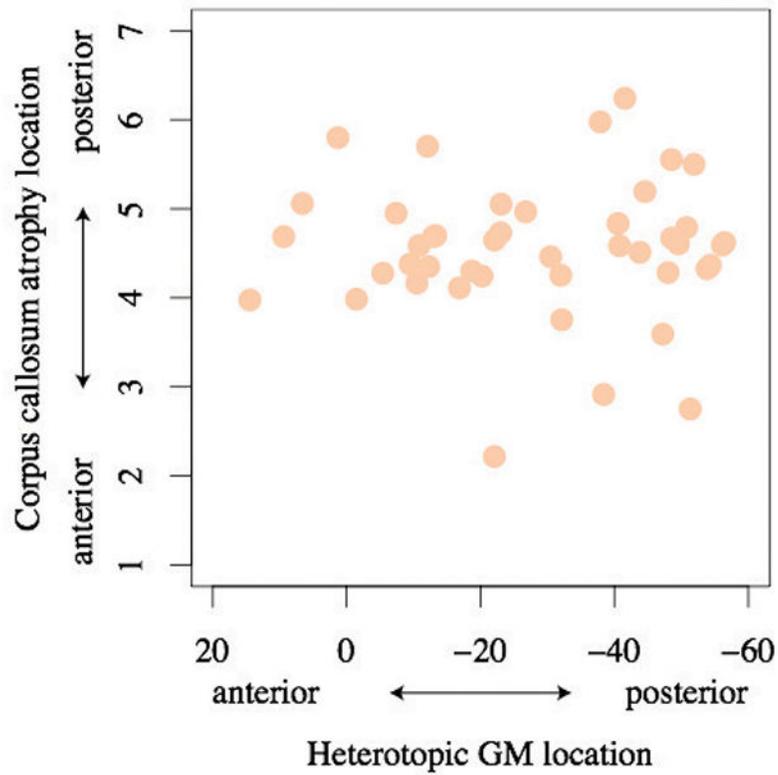
Figure 6.
No relationship was observed between the anterior-posterior distribution of heterotopic GM and the anterior-posterior distribution of corpus callosum atrophy (p = 0.92), suggesting that the position of heterotopic GM along the anterior-posterior axis does not determine the anterior-posterior position of corpus callosum atrophy.